Search for the B_c meson

P. Abreu, W. Adam, T. Adye, I. Ajinenko, G D. Alekseev, R. Alemany, P P. Allport, S. Almehed, S. Amato, A. Andreazza, et al.

EUROPEAN ORGANIZATION FOR NUCLEAR RESEARCH

CERN–PPE/96–194

18 December 1996

Search for the B_c Meson

DELPHI Collaboration

Abstract

In a sample of 3.02 million hadronic Z^o decays collected by the DELPHI detector, 270 $J/\psi \to \ell^+\ell^-$ candidates have been selected. A search for fully reconstructed ${B_c}^{\pm}$ mesons has yielded one ${B_c}^{\pm} \to J/\psi\ \pi^{\pm}$ candidate, no ${B_c}^{\pm} \to J/\psi\ \ell^{\pm}\ \nu_\ell$ candidates, and one ${B_c}^{\pm} \to J/\psi\ \pi^+\ \pi^-\ \pi^{\pm}$ candidate, consistent with expected background in each channel. The following 90% confidence level upper limits are determined:

$$Br(Z^o \to {B_c}^{\pm}\ X) \times Br({B_c}^{\pm} \to J/\psi\ \pi^{\pm}) < (1.05 \text{ to } 0.84) \times 10^{-4}$$

and

$$Br(Z^o \to {B_c}^{\pm}\ X) \times Br({B_c}^{\pm} \to J/\psi\ \ell^{\pm}\ \nu_\ell) < (5.8 \text{ to } 5.0) \times 10^{-5},$$

where the ranges quoted correspond to the range of predicted ${B_c}^{\pm}$ lifetimes from 0.4 to 1.4 ps, and

$$Br(Z^o \to {B_c}^{\pm}\ X) \times Br({B_c}^{\pm} \to J/\psi\ \pi^+\ \pi^-\ \pi^{\pm}) < 1.75 \times 10^{-4},$$

constant over the range of predicted ${B_c}^{\pm}$ lifetimes.

(To be submitted to Physics Letters B)

P.Abreu[21], W.Adam[50], T.Adye[37], I.Ajinenko[42], G.D.Alekseev[16], R.Alemany[49], P.P.Allport[22], S.Almehed[24], U.Amaldi[9], S.Amato[47], A.Andreazza[28], M.L.Andrieux[14], P.Antilogus[9], W-D.Apel[17], B.Åsman[44], J-E.Augustin[25], A.Augustinus[9], P.Baillon[9], P.Bambade[19], F.Barao[21], M.Barbi[47], G.Barbiellini[46], D.Y.Bardin[16], G.Barker[9], A.Baroncelli[40], O.Barring[24], J.A.Barrio[26], W.Bartl[50], M.J.Bates[37], M.Battaglia[15], M.Baubillier[23], J.Baudot[39], K-H.Becks[52], M.Begalli[6], P.Beilliere[8], Yu.Belokopytov[9,53], K.Belous[42], A.C.Benvenuti[5], M.Berggren[47], D.Bertini[25], D.Bertrand[2], M.Besancon[39], F.Bianchi[45], M.Bigi[45], M.S.Bilenky[16], P.Billoir[23], M-A.Bizouard[19], D.Bloch[10], M.Blume[52], T.Bolognese[39], M.Bonesini[28], W.Bonivento[28], P.S.L.Booth[22], G.Borisov[39,42], C.Bosio[40], O.Botner[48], E.Boudinov[31], B.Bouquet[19], C.Bourdarios[9], T.J.V.Bowcock[22], M.Bozzo[13], P.Branchini[40], K.D.Brand[36], T.Brenke[52], R.A.Brenner[15], C.Bricman[2], R.C.A.Brown[9], P.Bruckman[18], J-M.Brunet[8], L.Bugge[33], T.Buran[33], T.Burgsmueller[52], P.Buschmann[52], S.Cabrera[49], M.Caccia[28], M.Calvi[28], A.J.Camacho Rozas[41], T.Camporesi[9], V.Canale[38], M.Canepa[13], K.Cankocak[44], F.Cao[2], F.Carena[9], L.Carroll[22], C.Caso[13], M.V.Castillo Gimenez[49], A.Cattai[9], F.R.Cavallo[5], V.Chabaud[9], Ph.Charpentier[9], L.Chaussard[25], P.Checchia[36], G.A.Chelkov[16], M.Chen[2], R.Chierici[45], P.Chliapnikov[42], P.Chochula[7], V.Chorowicz[9], V.Cindro[43], P.Collins[9], R.Contri[13], E.Cortina[49], G.Cosme[19], F.Cossutti[46], J-H.Cowell[22], H.B.Crawley[1], D.Crennell[37], G.Crosetti[13], J.Cuevas Maestro[34], S.Czellar[15], E.Dahl-Jensen[29], J.Dahm[52], B.Dalmagne[19], M.Dam[29], G.Damgaard[29], P.D.Dauncey[37], M.Davenport[9], W.Da Silva[23], C.Defoix[8], A.Deghorain[2], G.Della Ricca[46], P.Delpierre[27], N.Demaria[35], A.De Angelis[9], W.De Boer[17], S.De Brabandere[2], C.De Clercq[2], C.De La Vaissiere[23], B.De Lotto[46], A.De Min[36], L.De Paula[47], C.De Saint-Jean[39], H.Dijkstra[9], L.Di Ciaccio[38], A.Di Diodato[38], F.Djama[10], A.Djannati[8], J.Dolbeau[8], K.Doroba[51], M.Dracos[10], J.Drees[52], K.-A.Drees[52], M.Dris[32], J-D.Durand[25,9], D.Edsall[1], R.Ehret[17], G.Eigen[4], T.Ekelof[48], G.Ekspong[44], M.Elsing[9], J-P.Engel[10], B.Erzen[43], M.Espirito Santo[21], E.Falk[24], D.Fassouliotis[32], M.Feindt[9], A.Fenyuk[42], A.Ferrer[49], S.Fichet[23], T.A.Filippas[32], A.Firestone[1], P.-A.Fischer[10], H.Foeth[9], E.Fokitis[32], F.Fontanelli[13], F.Formenti[9], B.Franek[37], P.Frenkiel[8], D.C.Fries[17], A.G.Frodesen[4], R.Fruhwirth[50], F.Fulda-Quenzer[19], J.Fuster[49], A.Galloni[22], D.Gamba[45], M.Gandelman[47], C.Garcia[49], J.Garcia[41], C.Gaspar[9], U.Gasparini[36], Ph.Gavillet[9], E.N.Gazis[32], D.Gele[10], J-P.Gerber[10], L.Gerdyukov[42], R.Gokieli[51], B.Golob[43], G.Gopal[37], L.Gorn[1], M.Gorski[51], Yu.Gouz[45,53], V.Gracco[13], E.Graziani[40], C.Green[22], A.Grefrath[52], P.Gris[39], G.Grosdidier[19], K.Grzelak[51], S.Gumenyuk[28,53], P.Gunnarsson[44], M.Gunther[48], J.Guy[37], F.Hahn[9], S.Hahn[52], Z.Hajduk[18], A.Hallgren[48], K.Hamacher[52], F.J.Harris[35], V.Hedberg[24], R.Henriques[21], J.J.Hernandez[49], P.Herquet[2], H.Herr[9], T.L.Hessing[35], J.-M.Heuser[52], E.Higon[49], H.J.Hilke[9], T.S.Hill[1], S-O.Holmgren[44], P.J.Holt[35], D.Holthuizen[31], S.Hoorelbeke[2], M.Houlden[22], J.Hrubec[50], K.Huet[2], K.Hultqvist[44], J.N.Jackson[22], R.Jacobsson[44], P.Jalocha[18], R.Janik[7], Ch.Jarlskog[24], G.Jarlskog[24], P.Jarry[39], B.Jean-Marie[19], E.K.Johansson[44], L.Jonsson[24], P.Jonsson[24], C.Joram[9], P.Juillot[10], M.Kaiser[17], F.Kapusta[23], K.Karafasoulis[11], M.Karlsson[44], E.Karvelas[11], S.Katsanevas[3], E.C.Katsoufis[32], R.Keranen[4], Yu.Khokhlov[42], B.A.Khomenko[16], N.N.Khovanski[16], B.King[22], N.J.Kjaer[31], O.Klapp[52], H.Klein[9], A.Klovning[4], P.Kluit[31], B.Koene[31], P.Kokkinias[11], M.Koratzinos[9], K.Korcyl[18], V.Kostioukhine[42], C.Kourkoumelis[3], O.Kouznetsov[13,16], M.Krammer[50], C.Kreuter[9], I.Kronkvist[24], Z.Krumstein[16], W.Krupinski[18], P.Kubinec[7], W.Kucewicz[18], K.Kurvinen[15], C.Lacasta[49], I.Laktineh[25], J.W.Lamsa[1], L.Lanceri[46], D.W.Lane[1], P.Langefeld[52], J-P.Laugier[39], R.Lauhakangas[15], G.Leder[50], F.Ledroit[14], V.Lefebure[2], C.K.Legan[1], R.Leitner[30], J.Lemonne[2], G.Lenzen[52], V.Lepeltier[19], T.Lesiak[18], J.Libby[35], D.Liko[9], R.Lindner[52], A.Lipniacka[44], I.Lippi[36], B.Loerstad[24], J.G.Loken[35], J.M.Lopez[41], D.Loukas[11], P.Lutz[39], L.Lyons[35], J.MacNaughton[50], G.Maehlum[17], J.R.Mahon[6], A.Maio[21], T.G.M.Malmgren[44], V.Malychev[16], F.Mandl[50], J.Marco[41], R.Marco[41], B.Marechal[47], M.Margoni[36], J-C.Marin[9], C.Mariotti[9], A.Markou[11], C.Martinez-Rivero[34], F.Martinez-Vidal[49], S.Marti i Garcia[22], F.Matorras[41], C.Matteuzzi[28], G.Matthiae[38], M.Mazzucato[36], M.Mc Cubbin[22], R.Mc Kay[1], R.Mc Nulty[22], J.Medbo[48], M.Merk[31], C.Meroni[28], S.Meyer[17], W.T.Meyer[1], A.Miagkov[42], M.Michelotto[36], E.Migliore[45], L.Mirabito[25], W.A.Mitaroff[50], U.Mjoernmark[24], T.Moa[44], R.Moeller[29], K.Moenig[9], M.R.Monge[13], P.Morettini[13], H.Mueller[17], K.Muenich[52], M.Mulders[31], L.M.Mundim[6], W.J.Murray[37], B.Muryn[14,18], G.Myatt[35], F.Naraghi[14], F.L.Navarria[5], S.Navas[49], K.Nawrocki[51], P.Negri[28], S.Nemecek[12], W.Neumann[52], R.Nicolaidou[3], B.S.Nielsen[29], M.Nieuwenhuizen[31], V.Nikolaenko[10], P.Niss[44], A.Nomerotski[36], A.Normand[35], M.Novak[12], W.Oberschulte-Beckmann[17], V.Obraztsov[42], A.G.Olshevski[16], A.Onofre[21], R.Orava[15], K.Osterberg[15], A.Ouraou[39], P.Paganini[19], M.Paganoni[9,28], P.Pages[10], R.Pain[23], H.Palka[18], Th.D.Papadopoulou[32], K.Papageorgiou[11], L.Pape[9], C.Parkes[35], F.Parodi[13], A.Passeri[40], M.Pegoraro[36], H.Pernegger[50], M.Pernicka[50], A.Perrotta[5], C.Petridou[46], A.Petrolini[13], H.T.Phillips[37], G.Piana[13], F.Pierre[39], M.Pimenta[21], T.Podobnik[43], O.Podobrin[9], M.E.Pol[6], G.Polok[18], P.Poropat[46], V.Pozdniakov[16], P.Privitera[38], N.Pukhaeva[16], A.Pullia[28], D.Radojicic[35], S.Ragazzi[28], H.Rahmani[32], J.Rames[12], P.N.Ratoff[20], A.L.Read[33], M.Reale[52], P.Rebecchi[19], N.G.Redaelli[28], M.Regler[50], D.Reid[9], R.Reinhardt[52], P.B.Renton[35], L.K.Resvanis[3], F.Richard[19], J.Richardson[22], J.Ridky[12], G.Rinaudo[45], I.Ripp[39], A.Romero[45], I.Roncagliolo[13], P.Ronchese[36], L.Roos[23], E.I.Rosenberg[1], P.Roudeau[19], T.Rovelli[5], W.Ruckstuhl[31], V.Ruhlmann-Kleider[39], A.Ruiz[41], K.Rybicki[18], H.Saarikko[15], Y.Sacquin[39], A.Sadovsky[16], O.Sahr[14], G.Sajot[14], J.Salt[49], J.Sanchez[26], M.Sannino[13], M.Schimmelpfennig[17], H.Schneider[17], U.Schwickerath[17], M.A.E.Schyns[52], G.Sciolla[45], F.Scuri[46], P.Seager[20], Y.Sedykh[16], A.M.Segar[35], A.Seitz[17], R.Sekulin[37], L.Serbelloni[38], R.C.Shellard[6], P.Siegrist[39], R.Silvestre[39], S.Simonetti[39], F.Simonetto[36], A.N.Sisakian[16], B.Sitar[7], T.B.Skaali[33], G.Smadja[25], N.Smirnov[42], O.Smirnova[24], G.R.Smith[37], O.Solovianov[42], R.Sosnowski[51], D.Souza-Santos[6], T.Spassov[21], E.Spiriti[40], P.Sponholz[52], S.Squarcia[13], D.Stampfer[9], C.Stanescu[40], S.Stanic[43], S.Stapnes[33], I.Stavitski[36], K.Stevenson[35], A.Stocchi[19], J.Strauss[50], R.Strub[10], B.Stugu[4], M.Szczekowski[51], M.Szeptycka[51],

T.Tabarelli[28], J.P.Tavernet[23], J.Thomas[35], A.Tilquin[27], J.Timmermans[31], L.G.Tkatchev[16], T.Todorov[10], S.Todorova[10], D.Z.Toet[31], A.Tomaradze[2], B.Tome[21], A.Tonazzo[28], L.Tortora[40], G.Transtromer[24], D.Treille[9], G.Tristram[8], A.Trombini[19], C.Troncon[28], A.Tsirou[9], M-L.Turluer[39], I.A.Tyapkin[16], M.Tyndel[37], S.Tzamarias[22], B.Ueberschaer[52], O.Ullaland[9], V.Uvarov[42], G.Valenti[5], E.Vallazza[9], C.Vander Velde[2], G.W.Van Apeldoorn[31], P.Van Dam[31], W.K.Van Doninck[2], J.Van Eldik[31], A.Van Lysebetten[2], N.Vassilopoulos[35], G.Vegni[28], L.Ventura[36], W.Venus[37], F.Verbeure[2], M.Verlato[36], L.S.Vertogradov[16], D.Vilanova[39], P.Vincent[25], L.Vitale[46], E.Vlasov[42], A.S.Vodopyanov[16], V.Vrba[12], H.Wahlen[52], C.Walck[44], M.Weierstall[52], P.Weilhammer[9], C.Weiser[17], A.M.Wetherell[9], D.Wicke[52], J.H.Wickens[2], M.Wielers[17], G.R.Wilkinson[9], W.S.C.Williams[35], M.Winter[10], M.Witek[18], T.Wlodek[19], K.Woschnagg[48], K.Yip[35], O.Yushchenko[42], F.Zach[25], A.Zaitsev[42], A.Zalewska[9], P.Zalewski[51], D.Zavrtanik[43], E.Zevgolatakos[11], N.I.Zimin[16], M.Zito[39], D.Zontar[43], G.C.Zucchelli[44], G.Zumerle[36]

[1] Department of Physics and Astronomy, Iowa State University, Ames IA 50011-3160, USA
[2] Physics Department, Univ. Instelling Antwerpen, Universiteitsplein 1, B-2610 Wilrijk, Belgium
and IIHE, ULB-VUB, Pleinlaan 2, B-1050 Brussels, Belgium
and Faculté des Sciences, Univ. de l'Etat Mons, Av. Maistriau 19, B-7000 Mons, Belgium
[3] Physics Laboratory, University of Athens, Solonos Str. 104, GR-10680 Athens, Greece
[4] Department of Physics, University of Bergen, Allégaten 55, N-5007 Bergen, Norway
[5] Dipartimento di Fisica, Università di Bologna and INFN, Via Irnerio 46, I-40126 Bologna, Italy
[6] Centro Brasileiro de Pesquisas Físicas, rua Xavier Sigaud 150, RJ-22290 Rio de Janeiro, Brazil
and Depto. de Física, Pont. Univ. Católica, C.P. 38071 RJ-22453 Rio de Janeiro, Brazil
and Inst. de Física, Univ. Estadual do Rio de Janeiro, rua São Francisco Xavier 524, Rio de Janeiro, Brazil
[7] Comenius University, Faculty of Mathematics and Physics, Mlynska Dolina, SK-84215 Bratislava, Slovakia
[8] Collège de France, Lab. de Physique Corpusculaire, IN2P3-CNRS, F-75231 Paris Cedex 05, France
[9] CERN, CH-1211 Geneva 23, Switzerland
[10] Centre de Recherche Nucléaire, IN2P3 - CNRS/ULP - BP20, F-67037 Strasbourg Cedex, France
[11] Institute of Nuclear Physics, N.C.S.R. Demokritos, P.O. Box 60228, GR-15310 Athens, Greece
[12] FZU, Inst. of Physics of the C.A.S. High Energy Physics Division, Na Slovance 2, 180 40, Praha 8, Czech Republic
[13] Dipartimento di Fisica, Università di Genova and INFN, Via Dodecaneso 33, I-16146 Genova, Italy
[14] Institut des Sciences Nucléaires, IN2P3-CNRS, Université de Grenoble 1, F-38026 Grenoble Cedex, France
[15] Research Institute for High Energy Physics, SEFT, P.O. Box 9, FIN-00014 Helsinki, Finland
[16] Joint Institute for Nuclear Research, Dubna, Head Post Office, P.O. Box 79, 101 000 Moscow, Russian Federation
[17] Institut für Experimentelle Kernphysik, Universität Karlsruhe, Postfach 6980, D-76128 Karlsruhe, Germany
[18] Institute of Nuclear Physics and University of Mining and Metalurgy, Ul. Kawiory 26a, PL-30055 Krakow, Poland
[19] Université de Paris-Sud, Lab. de l'Accélérateur Linéaire, IN2P3-CNRS, Bât. 200, F-91405 Orsay Cedex, France
[20] School of Physics and Chemistry, University of Lancaster, Lancaster LA1 4YB, UK
[21] LIP, IST, FCUL - Av. Elias Garcia, 14-1°, P-1000 Lisboa Codex, Portugal
[22] Department of Physics, University of Liverpool, P.O. Box 147, Liverpool L69 3BX, UK
[23] LPNHE, IN2P3-CNRS, Universités Paris VI et VII, Tour 33 (RdC), 4 place Jussieu, F-75252 Paris Cedex 05, France
[24] Department of Physics, University of Lund, Sölvegatan 14, S-22363 Lund, Sweden
[25] Université Claude Bernard de Lyon, IPNL, IN2P3-CNRS, F-69622 Villeurbanne Cedex, France
[26] Universidad Complutense, Avda. Complutense s/n, E-28040 Madrid, Spain
[27] Univ. d'Aix - Marseille II - CPP, IN2P3-CNRS, F-13288 Marseille Cedex 09, France
[28] Dipartimento di Fisica, Università di Milano and INFN, Via Celoria 16, I-20133 Milan, Italy
[29] Niels Bohr Institute, Blegdamsvej 17, DK-2100 Copenhagen 0, Denmark
[30] NC, Nuclear Centre of MFF, Charles University, Areal MFF, V Holesovickach 2, 180 00, Praha 8, Czech Republic
[31] NIKHEF, Postbus 41882, NL-1009 DB Amsterdam, The Netherlands
[32] National Technical University, Physics Department, Zografou Campus, GR-15773 Athens, Greece
[33] Physics Department, University of Oslo, Blindern, N-1000 Oslo 3, Norway
[34] Dpto. Fisica, Univ. Oviedo, Avda. Calvo Sotelo, S/N-33007 Oviedo, Spain, (CICYT-AEN96-1681)
[35] Department of Physics, University of Oxford, Keble Road, Oxford OX1 3RH, UK
[36] Dipartimento di Fisica, Università di Padova and INFN, Via Marzolo 8, I-35131 Padua, Italy
[37] Rutherford Appleton Laboratory, Chilton, Didcot OX11 OQX, UK
[38] Dipartimento di Fisica, Università di Roma II and INFN, Tor Vergata, I-00173 Rome, Italy
[39] CEA, DAPNIA/Service de Physique des Particules, CE-Saclay, F-91191 Gif-sur-Yvette Cedex, France
[40] Istituto Superiore di Sanità, Ist. Naz. di Fisica Nucl. (INFN), Viale Regina Elena 299, I-00161 Rome, Italy
[41] Instituto de Fisica de Cantabria (CSIC-UC), Avda. los Castros, S/N-39006 Santander, Spain, (CICYT-AEN96-1681)
[42] Inst. for High Energy Physics, Serpukov P.O. Box 35, Protvino, (Moscow Region), Russian Federation
[43] Department of Astroparticle Physics, School of Environmental Sciences, Nova Gorica, and J. Stefan Institute, Ljubljana, Slovenia
[44] Fysikum, Stockholm University, Box 6730, S-113 85 Stockholm, Sweden
[45] Dipartimento di Fisica Sperimentale, Università di Torino and INFN, Via P. Giuria 1, I-10125 Turin, Italy
[46] Dipartimento di Fisica, Università di Trieste and INFN, Via A. Valerio 2, I-34127 Trieste, Italy
and Istituto di Fisica, Università di Udine, I-33100 Udine, Italy
[47] Univ. Federal do Rio de Janeiro, C.P. 68528 Cidade Univ., Ilha do Fundão BR-21945-970 Rio de Janeiro, Brazil
[48] Department of Radiation Sciences, University of Uppsala, P.O. Box 535, S-751 21 Uppsala, Sweden
[49] IFIC, Valencia-CSIC, and D.F.A.M.N., U. de Valencia, Avda. Dr. Moliner 50, E-46100 Burjassot (Valencia), Spain
[50] Institut für Hochenergiephysik, Österr. Akad. d. Wissensch., Nikolsdorfergasse 18, A-1050 Vienna, Austria
[51] Inst. Nuclear Studies and University of Warsaw, Ul. Hoza 69, PL-00681 Warsaw, Poland
[52] Fachbereich Physik, University of Wuppertal, Postfach 100 127, D-42097 Wuppertal, Germany
[53] On leave of absence from IHEP Serpukhov

1 Introduction

With around 3 million hadronic Z^0 decays recorded by each LEP experiment, the properties of B mesons having a constituent b-quark partnered by one light uds quark have been well determined from various decay channels. While a wealth of $c\overline{c}$ and $b\overline{b}$ states are known, no hadron with two heavy quarks of different flavours has so far been observed.

Predictions of the $B_c^{\pm}$ ground state masses are based on potential models [1–5]. In a survey of techniques for estimating masses, Kwong and Rosner [2] indicate a range of 6.194 to 6.292 GeV/c^2 for the mass of the $B_c^{\pm}$ ground state. More recently Quigg and Eichten [3] have calculated the mass to be 6.258 ± 0.020 GeV/c^2, while Bagan et al. [4] find 6.255 ± 0.020 GeV/c^2. A search for the $B_c^{\pm}$ meson via a fully reconstructed decay channel such as $J/\psi\pi$ between 6.0 and 6.5 GeV/c^2 would cover all possibilities.

The rate of $B_c^{\pm}$ meson production in $Z^0 \rightarrow b\overline{b}$ events via soft fragmentation cannot be very large as the relative probability of creating a $(u\overline{u})$ pair from the vacuum is 10^{10} to 10^{11} times that for a $(c\overline{c})$ pair [5]. Production of $B_c^{\pm}$ via its direct coupling to a virtual W boson is strongly suppressed as the CKM matrix element V_{cb} is small (0.036 to 0.046)[6]. The dominant production mechanism is when one of the primary b-quarks in a $Z^0 \rightarrow b\overline{b}$ event emits a hard virtual gluon which fragments to a $c\overline{c}$ and the $c(\overline{c})$ quark forms a bound state with a primary $\overline{b}(b)$ quark. The amplitude of this process is proportional to the wave function of the $B_c^{\pm}$ at the origin [1]. The branching fraction $Br(Z^0 \rightarrow B_c^{\pm}\ X)$ for the ground state is calculated to be $(1.0 - 4.5) \times 10^{-4}$ (including decays from the 1S and 2S states) [7,8]. The alternative, of a $b\overline{b}$ pair produced from gluon splitting in $Z^0 \rightarrow c\overline{c}$ events, is predicted to be a factor $(m_b/m_c)^3$ lower [7]).

Excited states of the $B_c^{\pm}$ should also be produced. Those with mass above the BD threshold ($>$ 7.15 GeV/c^2) will dissociate into a pair of B and D mesons and will not contribute to the inclusive $B_c^{\pm}$ production rate, but the 15 excited states expected below the BD threshold will decay to the ground state $B_c^{\pm}$ either via hadronic cascades or by photon emission [9]. The branching fractions $Br(Z^0 \rightarrow B_c^*\ X)$ for the 2P and 3P states have been calculated [10,11] to be $(0.2 - 1.2) \times 10^{-4}$. For completeness, the small expected contributions from the D-wave and F-wave states with masses below the BD threshold should also be included. With the P-wave states decaying to the ground state, the overall branching fraction $Br(Z^0 \rightarrow B_c^{\pm}\ X)$ is expected to be $(1.2 - 5.7) \times 10^{-4}$.

The $B_c^{\pm}$ can decay via the decay of the b or the c quark, or via the weak annihilation of the $b\bar{c}$ $(c\bar{b})$ quark-antiquark pair. The decay widths corresponding to the three mechanisms have been estimated in potential models and using QCD sum rules [12]:

	b-decay	c-decay	annihilation
Potentials	37%	45%	18%
Sum rules	48%	39%	13%

Neglecting the annihilation channel, the lifetime of the $B_c^{\pm}$ can be estimated [13] from

$$\frac{1}{\tau_{B_c}} = \frac{1}{\tau_B} + \frac{1}{\tau_D}.$$

The measured values of τ_{B^+} and τ_{D^+} then give $\tau_{B_c^+} = 0.6$ ps. However it has been argued [9] that, as the $B_c^{\pm}$ is a tightly bound system, the decay width should be expressed in terms of effective quark masses reduced by the binding energy. Depending on the value of this correction, the lifetime of the $B_c^{\pm}$ could range from $(0.4 - 1.4)$ ps [9,13,14].

The deep binding between b and c quarks suggests that decays to final states including J/ψ will be prominent; however, the uncertainty in the expected branching fraction for any specific decay channel is considerable [15]. The predicted inclusive branching fraction for $B_c^{\pm} \rightarrow J/\psi\ X^{\pm}$ ranges between 10% and 24% [14,15].

The present search is restricted to the channels that give the clearest signature for $B_c^{\pm}$ mesons. These are

$$B_c^{\pm} \rightarrow J/\psi\ \pi^{\pm} \quad (1)$$
$$B_c^{\pm} \rightarrow J/\psi\ e^{\pm}\nu_e \quad (2)$$
$$B_c^{\pm} \rightarrow J/\psi\ \mu^{\pm}\nu_{\mu} \quad (3)$$
$$B_c^{\pm} \rightarrow J/\psi\ (3\pi)^{\pm} \quad (4)$$

The predicted decay branching ratios for these channels range from 0.2%-2% for channel (1), and from 1% to 5% for channels (2) and (3) [14,12,15]. There are no theoretical predictions for the branching ratio for channel (4). However, by comparison with the decay branching ratios for $B^0 \rightarrow D^{*\pm}\pi^{\mp}$ and $B^0 \rightarrow D^{*\pm}3\pi^{\mp}$, one would expect it to be of comparable strength to channel (1).

The decay of the J/ψ to a pair of oppositely charged leptons of the same flavour selects an almost background-free sample of B-hadrons decaying to J/ψ. In the semileptonic decay channel, the presence of a third lepton in geometrical correlation with the two leptons from the J/ψ decay signals the existence of $B_c^{\pm}$. Observation of a signal in this channel would enable the production rate to be estimated. Detection of $B_c^{\pm} \rightarrow J/\psi\ \pi^{\pm}$ and $B_c^{\pm} \rightarrow J/\psi\ 3(\pi)^{\pm}$ would allow the mass to be determined.

The detailed description of the various DELPHI components and of their performance can be found in [16,17]. Section 2 of this paper describes the selection of hadronic events containing a J/ψ candidate decaying to a pair of same-flavour opposite-sign leptons. The vertex reconstruction procedure used to improve the purity of the J/ψ sample is described in section 3. The $B_c^{\pm}$ candidate selection for each of the channels is described in section 4. Section 5 summarises the conclusions.

2 Event Selection

The search for the $B_c^{\pm}$ meson was performed on the data and on fully simulated and reconstructed event samples: a general $Z^0 \rightarrow q\bar{q}$ sample (not including $B_c^{\pm}$ production) to determine the background, and signal events for each of the four channels and both J/ψ decay modes in order to determine the efficiency of observing the signal. The B-hadron decay lifetime used in these simulated events was 1.6 ps, and the $B_c^{\pm}$ meson mass was 6250 MeV/c^2 .

2.1 Hadronic Events

From the data recorded by DELPHI in the years 1991 to 1994, the events with 5 or more charged particles were selected as hadronic Z^0 decays. Each accepted charged particle was required to have:

- measured momentum (p) greater than 200 MeV/c,
- momentum error δp less than p,
- impact parameter transverse to the beam below 2.5 cm and
- impact parameter along the beam below 10.0 cm.

A further requirement was that the components of the detector crucial to this analysis, namely the Vertex Detector (VD), the Tracking Detectors, the electromagnetic calorimeters for electron identification and the muon chambers outside the magnet return yoke, be fully operational. For charged particle identification, information from the Ring Imaging Cherenkov (RICH) detectors and on the ionisation loss rate (dE/dX) in the Time Projection Chamber (TPC) were used when available.

A total of 3.02×10^6 hadronic events were selected from the data. For background estimation, a total of 7.76×10^6 fully reconstructed $Z^0 \to q\overline{q}$ simulated hadronic events (excluding the small number generated with a $B_c^{\pm}$) were selected. The simulation sample, containing 5077 events with at least one J/ψ decaying to $\ell^+\ell^-$ in the final state, allowed for the time variation of the detector geometry, alignment, analysis software, and calibration over the 1991 to 1994 data taking period. All numbers of background simulation events quoted henceforth are

- normalised to the total number of hadronic events in the data and
- corrected for the differences between the branching ratios $Br(Z^0 \to J/\psi X)$, $Br(J/\psi \to \mu^+\mu^-)$ and $Br(J/\psi \to e^+e^-)$ used in the simulation and the current measured values [6].

The numbers of signal events generated for the channels under study are given in Table 1.

2.2 J/ψ Selection

The main background to B meson decays to J/ψ comes from cascade semileptonic decays of the b-quark followed by the c-quark. The small prompt J/ψ production is eliminated by requiring a significant flight distance of the J/ψ from the primary interaction point.

For each selected event, the thrust axis was determined using all charged particles passing the cuts described above and the energy depositions, identified as photons, in the electromagnetic calorimeters. The plane perpendicular to the thrust axis split the event into two hemispheres. Candidate $J/\psi \to \ell^+\ell^-$ were required to have two well measured, oppositely charged, same-flavour identified leptons, in the same hemisphere and having a combined mass within the range 2.5 to 3.5 GeV/c^2. The muon and electron identification criteria used in DELPHI are described in [17]. A more detailed study of J/ψ production can be found in [18].

In total, 2420 events were selected from the data and 2665 events from the general $Z^0 \to q\overline{q}$ simulation sample. The efficiency of selecting true $J/\psi \to \ell^+\ell^-$ was 37% with a purity of 26%. The numbers of events selected from the signal simulation samples are given in Table 1.

3 Vertex Reconstruction and Background Reduction

To increase the signal to background ratio for $J/\psi \to \ell^+\ell^-$ events, the primary and J/ψ vertices were reconstructed. The analysis was restricted to events with each J/ψ decay lepton having momentum (P_ℓ) greater than 2.0 GeV/c, as the lepton identification efficiency is fairly uniform above this momentum. Since the analysis depends on good primary and secondary vertices, the charged particle tracks used in the reconstruction were required to have at least a certain minimum number of associated hits in the VD.

This minimum number was defined to be two in the $R\Phi$ plane for 1991 to 1993, when the three layers of the VD supplied only $R\Phi$ information, and at least one in $R\Phi$ and one in Z for 1994, when two of the three planes provided Z information as well. Vertex reconstruction was done in the $R\Phi$ plane for the 1991 to 1993 data and in 3D for the 1994 data.

3.1 Primary Vertex

All charged particle tracks, excluding those of the leptons from the J/ψ decay, were used for primary vertex reconstruction if they had sufficient associated hits in the VD.

The vertex reconstruction procedure used was iterative, starting with all selected tracks being constrained in the fit to pass through the known beam spot with its errors. The contribution to the fit χ^2 from any participating track was required to be less than 3.5 when fitting in $R\Phi$ only, and 5.25 when fitting in 3D. The track with the largest χ^2 contribution, if it was greater than this value, was removed and the fit redone. This iterative procedure ended when the largest χ^2 contribution was below the allowed limit, or when only one track remained. In the latter case the event was rejected.

If the probability of the resulting vertex fit was less than 0.1%, the track with the largest contribution to the χ^2 was removed and the vertex refitted. This second iterative procedure ended when the vertex fit had a χ^2 probability greater than 0.1% with at least two tracks. In all, 6% of the events had no successful primary vertex fit and were rejected.

3.2 Secondary Vertex

The crossing point of the lepton tracks of the J/ψ decay was used as the starting point for the secondary vertex. In the same hemisphere, further tracks were selected if they

- had the required minimum number of associated hits in the VD, and
- gave a χ^2 contribution of less than 3.0 in the $R\Phi$ plane, or 4.0 in 3D, when fitting to a common vertex with the two lepton tracks from the J/ψ decay.

All the tracks thus identified as originating from the J/ψ decay point were then used to reconstruct the secondary vertex. If the χ^2 probability of the resulting fit was below 0.1%, the track (excluding the two lepton tracks) with the largest χ^2 contribution was removed and the fit redone. This iterative procedure was stopped when a fit with at least three tracks (including the two lepton tracks) had a χ^2 probability above 0.1%. In events with no successful vertex fit with at least three tracks, the crossing point (vertex in 3D) of the two lepton tracks was accepted as the secondary vertex.

Events were accepted for further analysis only if the scalar product of the J/ψ momentum vector and the direction vector from the primary to the secondary vertex was found to be positive.

Successful secondary vertex reconstruction reduced the non-$b\bar{b}$ background considerably. The purity of the $J/\psi \rightarrow \ell^+\ell^-$ sample, estimated from the fully reconstructed simulation sample, increased from 26% to around 44%, without any decay length cut.

To reduce the background further

- the distance between the primary and secondary vertices ($L_{J/\psi}$) was required to be greater than twice the error on this distance, and
- the difference (ΔM) between the combined mass ($M_{\ell^+\ell^-}$) of the pair of oppositely charged same-flavour leptons and the central value (found to be consistent with the world average J/ψ mass [6]) had to be

- consistent with zero within three times its error, and
- within the range -100 to $+100$ MeV/c^2 for di-muons and -300 to $+100$ MeV/c^2 for di-electrons, to remove badly measured events.

A total of 270 events were selected from the data, compared to 300 in the simulation sample. The purity of the $J/\psi \rightarrow \ell^+\ell^-$ sample increased to 77% and the efficiency decreased to 16%. The numbers of simulated signal events passing the various selections described so far are given in Table 1.

Table 1: Simulated $B_c^{\pm} \rightarrow J/\psi\ X^{\pm}$ events at different stages of the analysis

$B_c^{\pm} \rightarrow J/\psi\ +$	$\pi^{\pm}$		$e^{\pm}\ \nu_e$		$\mu^{\pm}\ \nu_\mu$		$\pi^+\pi^-\pi^{\pm}$	
$J/\psi \rightarrow$	$\mu^+\mu^-$	e^+e^-	$\mu^+\mu^-$	e^+e^-	$\mu^+\mu^-$	e^+e^-	$\mu^+\mu^-$	e^+e^-
Generated	1225	1353	1331	1332	1259	1276	835	931
Selected $J/\psi \rightarrow \ell^+\ell^-$	672	303	694	346	716	273	448	202
$P_\ell > 2.0$ GeV/c	551	253	569	285	613	214	366	162
Good Primary Vertex	517	240	538	278	587	207	350	158
Good Secondary Vertex	323	173	332	217	332	143	224	129
$L_{J/\psi} > 2\sigma(L_{J/\psi})$	301	166	294	211	306	134	207	125
ΔM Cut	271	130	260	150	253	104	187	96

4 $B_c^{\pm}$ Candidate Selections

For the $B_c^{\pm} \rightarrow J/\psi\ \pi^{\pm}$ and $B_c^{\pm} \rightarrow J/\psi\ \ell^{\pm}\nu_\ell$ candidates, at least one extra charged particle was required to be associated with the lepton pair from the J/ψ decay at the secondary vertex. At least three other charged particles were required for $B_c^{\pm} \rightarrow J/\psi\ (3\pi)^{\pm}$.

A charged particle in the same hemisphere as the J/ψ was associated to the secondary vertex if its track

- was used in the reconstruction of the secondary vertex, or
- had an impact parameter (in the $R\Phi$ plane) to the secondary vertex that
  - was less than 1 mm and less than three times its error, and
  - when normalised by its error, was no more than a factor two bigger than the normalised impact parameter to the primary vertex.

All charged particles thus associated to the secondary vertex were used in the mass reconstruction to search for the $B_c^{\pm}$ meson.

The requirement that the distance between the reconstructed primary and secondary vertices be greater than twice the error on this distance could reduce the $B_c^{\pm}$ selection efficiency for low values of the $B_c^{\pm}$ lifetime. The selection efficiencies were therefore determined as a function of the $B_c^{\pm}$ lifetime.

4.1 $B_c^{\pm} \rightarrow J/\psi\ \pi^{\pm}$

An event passing the cuts described was selected as a possible candidate if one of the charged particles associated with the J/ψ at the secondary vertex satisfied the following conditions:

- the particle was not identified as a lepton,
- the Ring Imaging Cherenkov (RICH) or ionization (dE/dX) measurements were consistent with the expectation for a pion (when neither dE/dX nor RICH information was available, the particle was tried both as a pion and a kaon in mass combinations with the J/ψ),
- the mass of the $(J/\psi\pi)$ combination calculated at the secondary vertex was between 6.0 and 6.5 GeV/c^2 for events where the J/ψ decayed to a pair of oppositely charged muons, or between 5.8 and 6.7 GeV/c^2 for events with J/ψ decaying to a pair of oppositely charged electrons.

The reconstructed $(J/\psi\ \pi^{\pm})$ mass distributions are shown in Fig. 1. One candidate event for each J/ψ decay mode ($\rightarrow e^+e^-$ and $\rightarrow \mu^+\mu^-$) can be seen in the appropriate mass window in the data, while there are 2.6 and 2.3 events respectively in the background simulated samples.

To eliminate spurious $(J/\psi\ \pi)$ combinations, the angle $\Delta(\phi)$ between the line joining the primary and secondary vertices and the momentum vector of the combination, projected onto the $R\Phi$ plane, was required to be less than 10°. From the $\Delta(\phi)$ distributions shown in Fig. 2, it can be seen that both the data events survive this cut, while the numbers of simulated background events are reduced to 2.0 and 1.4 respectively.

The measured B_u and B_d production rate in Z^0 hadronic decays is two orders of magnitude higher than the highest predicted rate for $B_c{}^{\pm}$ production. $B_c{}^{\pm}$ candidates were therefore required to have no mass combinations of particles at the secondary vertex compatible with the following B_u and B_d decays:

- $B_u^{\pm}\rightarrow J/\psi\ K^{\pm}\ (n\pi^{\pm})^0$ where $n = 0$, 2 or 4
- $B_u^{\pm}\rightarrow J/\psi\ K^0\ (n\pi^{\pm})^{\pm}$, $n = 1$, 3 or 5
- $B_d^0\rightarrow J/\psi\ K^{\pm}\ (n\pi^{\pm})^{\mp}$, $n = 1$, 3 or 5
- $B_d^0\rightarrow J/\psi\ K^0\ (n\pi^{\pm})^0$, $n = 0$, 2 or 4.

In testing for these states, the charged kaon and the n charged pions were required to be associated to the secondary vertex and identified by the dE/dX and RICH information. A neutral kaon in the same hemisphere as the J/ψ was used in such invariant mass calculations only if its momentum vector was consistent with it originating from the secondary vertex. The typical mass resolution for these combinations was in the range $35 - 45$ MeV/c^2.

If the mass of such a combination, M$(J/\psi\ K\ n\pi)$, was found to be close to the known B_u or B_d mass [6] (ie within three times its error and within 100 MeV/c^2), the event was rejected if the angle $\Delta(\phi)$ for this combination of particles was less than 10°.

The two events selected from the data have measured $M(J/\psi\pi)$ masses of 6260 ± 131 MeV/c^2 and 6345 ± 85 MeV/c^2 and angles $\Delta(\phi)$ of 2.1° and 2.5° respectively. The first of these events has a valid interpretation as a $B_d\rightarrow J/\psi\ K^-\ \pi^+$ candidate, with M$(J/\psi\ K^-\ \pi^+) = 5318\pm116$ MeV/c^2 . A kinematic fit to the remaining candidate, with the three particles constrained to go through a common vertex and the mass of the di-muon pair constrained to the J/ψ mass, gave M$(J/\psi\ \pi^-) = 6341\pm27$ MeV/c^2 and a proper decay time of 0.38 ± 0.06ps. The numbers of background events surviving this anti-selection procedure are 1.1 and 0.6 in the two J/ψ decay modes.

The numbers of $B_c{}^{\pm}$ candidates selected from the two sets of signal simulation samples are given in Table 2, along with the selection efficiencies for the minimum and maximum predicted lifetimes of 0.4 ps and 1.4 ps respectively.

For both J/ψ decay modes, the $B_c{}^{\pm}$ selection efficiencies were found to increase linearly over the predicted range of $B_c{}^{\pm}$ lifetime. With one candidate, consistent with

Table 2: Numbers of simulated signal events selected and $B_c^{\pm} \to J/\psi\ X^{\pm}$ selection efficiency

$B_c^{\pm} \to J/\psi\ +$	$\pi^{\pm}$		$\pi^+\pi^-\pi^{\pm}$	
$J/\psi \to$	$\mu^+\mu^-$	e^+e^-	$\mu^+\mu^-$	e^+e^-
M($J/\psi\ X$) in Mass Window	155	66	59	32
$\Delta(\phi) < 10^\circ$	138	57	55	30
Without a $B_{u/d}$ combination	130	51	44	18
Selection efficiency for $\tau_{B_c} = 0.4$ ps	0.090±0.010	0.031±0.006	0.053±0.008	0.019±0.005
Selection efficiency for $\tau_{B_c} = 1.4$ ps	0.112±0.010	0.039±0.005	0.053±0.008	0.019±0.005

the expected background, and using $Br(J/\psi \to \ell^+\ell^-) = (12.03 \pm 0.27)\%$ [6] and these selection efficiencies, the 90% confidence level upper limit is

$$Br(Z^0 \to B_c^{\pm}\ X) \times Br(B_c^{\pm} \to J/\psi\ \pi^{\pm}) < (1.05 \text{ to } 0.84) \times 10^{-4},$$

where the range quoted corresponds to the predicted $B_c^{\pm}$ lifetime range from 0.4 to 1.4 ps.

4.2 $B_c^{\pm} \to J/\psi\ \pi^+\ \pi^-\ \pi^{\pm}$

Candidates for this decay channel were required to have at least 3 charged particles. Each of these was required to satisfy the same criteria as the single pion in the $J/\psi\ \pi^{\pm}$ channel (see section 4.1).

The reconstructed $(J/\psi\ (3\pi)^{\pm})$ mass distributions are shown in Fig. 3. The angle $\Delta(\phi)$ for each $J/\psi\ (3\pi)^{\pm}$ combination with mass within the search window is shown in Fig. 4. With the requirement that $\Delta(\phi)$ be less than 10° and that there be no B_u/B_d particle combinations with masses consistent with the known B_u/B_d mass, one event with $J/\psi \to \mu^+\mu^-$ is selected from the data, while 0.9 events with $J/\psi \to e^+e^-$ and 1.4 with $J/\psi \to \mu^+\mu^-$ are selected from the simulated background sample. A kinematic fit to the candidate gives M($J/\psi\pi^-\pi^-\pi^+$) = 6119 ± 22 MeV/c^2 and a proper decay time of 0.41 ± 0.07 ps. Since this mass is significantly different from that of the candidate found in the $J/\psi\ \pi^{\pm}$ channel, at least one of the two must be background.

The numbers of $B_c^{\pm}$ candidates selected from the two signal simulation samples and the selection efficiencies are given in Table 2. For both the J/ψ decay samples, the efficiencies are found to be uniform over the range of predicted $B_c^{\pm}$ lifetimes. With one candidate event found in the data, consistent with the expected background, the upper limit at the 90% confidence level is

$$Br(Z^0 \to B_c^{\pm}\ X) \times Br(B_c^{\pm} \to J/\psi\ \pi^+\ \pi^-\ \pi^{\pm}) < 1.75 \times 10^{-4},$$

uniform over the range of expected $B_c^{\pm}$ lifetimes.

4.3 $B_c^{\pm} \to J/\psi\ \ell^{\pm}\ \nu_\ell$

Candidates were selected from events passing the cuts described in the earlier sections and having one of the charged particle tracks associated with the J/ψ at the secondary vertex identified as a lepton. The particle selected as the third lepton also had to have momentum greater than 2.0 GeV/c.

With the probability of misidentifying a hadron as a lepton at around 1%, the background to these channels can come from combinations of any of the three leptons being

a misidentified hadron. The high J/ψ selection purity achieved by requiring a successfully reconstructed secondary vertex suggests that the predominant background originates from the association of a J/ψ with either a hadron (from the parent B decay or prompt) misidentified as a lepton, or a lepton originating from the primary interaction (i.e. not having a B parent).

Only one data event having a $J/\psi \rightarrow \mu^+\mu^-$ decay and a tagged electron satisfied the requirements. The invariant mass of the J/ψ and the lepton, M($J/\psi e^+$), is 4.027 $\pm$ 0.042 GeV/c^2. The reconstructed M($J/\psi\ell^\pm$) distributions for the simulated background events are shown in Figs. 5 a) and b). In the signal simulation samples, shown in Figs. 5 c) and d), 88% of the events have M($J/\psi\ell^\pm$) greater than 4.0 GeV/c^2, while only one background simulated event, with $J/\psi \rightarrow e^+e^-$, has M($J/\psi\mu^+$) above this value.

Events having M($J/\psi\ell^\pm$) greater than 4.0 GeV/c^2 and positive missing energy[†] in the hemisphere containing the J/ψ $\ell^\pm$ were selected as $B_c^\pm \rightarrow J/\psi$ $\ell^\pm$ ν_ℓ decay candidates. The single data event selected has negative missing energy in the J/ψ hemisphere. In the simulated background, 0.3 events (in the $J/\psi \rightarrow e^+e^-$ sample) have positive missing energy.

As before, the events were required to have no combination of appropriate particles with a mass consistent with the known B_u and B_d masses. The background expected from the simulation was unchanged.

Table 3: Numbers of simulated signal events selected and $B_c^\pm \rightarrow J/\psi$ $\ell^\pm$ ν_ℓ selection efficiency

$B_c^\pm \rightarrow J/\psi$ +	$e^\pm$ ν_e		$\mu^\pm$ ν_μ	
$J/\psi \rightarrow$	$\mu^+\mu^-$	e^+e^-	$\mu^+\mu^-$	e^+e^-
M($J/\psi\ell$) > 4.0 GeV/c^2 and $E_\nu > 0$	62	31	95	45
Without a $B_{u/d}$ combination	61	30	92	42
Selection efficiency for τ_{B_c}=0.4 ps	0.039±0.006	0.017±0.004	0.064±0.008	0.033±0.005
Selection efficiency for τ_{B_c}=1.4 ps	0.049±0.007	0.023±0.004	0.075±0.008	0.033±0.005

The numbers of signal simulated events selected are given in Table 3 along with the selection efficiencies. The mean efficiencies are again found to increase linearly with the $B_c^\pm$ lifetime.

With no $B_c^\pm \rightarrow J/\psi$ $e^\pm$ ν_e or $B_c^\pm \rightarrow J/\psi$ $\mu^\pm$ ν_μ candidates found in the data, the upper limits at 90% confidence level are

$$Br(Z^0 \rightarrow B_c^\pm\ X) \times Br(B_c^\pm \rightarrow J/\psi\ e^\pm\ \nu_e) < (1.61 \text{ to } 1.26) \times 10^{-4}$$

and

$$Br(Z^0 \rightarrow B_c^\pm\ X) \times Br(B_c^\pm \rightarrow J/\psi\ \mu^\pm\ \nu_\mu) < (0.98 \text{ to } 0.91) \times 10^{-4}$$

over the predicted $B_c^\pm$ lifetime range.

Combining the two channels, the 90% confidence level upper limits for τ_{B_c} = (0.4 to 1.4) ps are

$$Br(Z^0 \rightarrow B_c^\pm\ X) \times Br(B_c^\pm \rightarrow J/\psi\ \ell^\pm\ \nu_\ell) < (5.8 \text{ to } 5.0) \times 10^{-5}.$$

[†]The missing energy is calculated by subtracting the visible energy from the total energy in the hemisphere (beam energy corrected by the two hemisphere invariant masses). The visible energy is the sum of the energies of all charged particles measured by the tracking detectors and the photons measured by the electromagnetic calorimeters.

5 Conclusions

With one candidate found in the $B_c^{\pm} \to J/\psi\ \pi^{\pm}$ channel when 1.7 are expected from the background, an experimental 90% confidence level upper limit for the product of the $Z^0 \to B_c^{\pm}\ X^{\mp}$ production rate and the $B_c^{\pm} \to J/\psi\ \pi^{\pm}$ decay branching fraction has been determined to be 1.05×10^{-4} for a mean $B_c^{\pm}$ lifetime of $\tau_{B_c} = 0.4$ ps, decreasing linearly to 0.84×10^{-4} for $\tau_{B_c} = 1.4$ ps. This is an order of magnitude higher than the most optimistic theoretical estimate for this product. Similar limits have been reported by other LEP collaborations [19,20].

For the channel $B_c^{\pm} \to J/\psi\ \pi^+\ \pi^-\ \pi^{\pm}$, one candidate event found in the data is consistent with the 2.3 expected from the background. The corresponding upper limit, at the 90% confidence level, has been determined to be 1.75×10^{-4}, independent of the mean $B_c^{\pm}$ lifetime.

The reconstructed masses of the candidates in the two above channels are significantly different, suggesting that at least one of them is not a $B_c^{\pm}$ meson.

With no candidates seen in either $B_c^{\pm} \to J/\psi\ \ell^{\pm}\ \nu_\ell$ decay channel and 0.3 expected from the background, the combined 90% confidence level upper limit for the product of the $Z^0 \to B_c^{\pm}\ X^{\mp}$ production rate and the decay branching fraction has been determined to range from 5.8×10^{-5} to 5.0×10^{-5}. This is consistent with the optimistic theoretical estimate for this channel and with the limits reported by other LEP collaborations [19,21].

Acknowledgements

We are greatly indebted to our technical collaborators and to the funding agencies for their support in building and operating the DELPHI detector, and to the members of the CERN-SL Division for the excellent performance of the LEP collider.

References

[1] E. Eichten et al., Phys. Rev. **D17** (1978) 3090 and
Phys. Rev. **D21** (1980) 203; ibid. **D21** (1980) 313-E;
W. Buchmüller and S.-H.H.Tye, Phys. Rev. **D24** (1981) 132.
A. Martin, Phys. Lett. **B93** (1980) 338.
C. Quigg and J.L. Rosner, Phys. Lett. **B71** (1977) 153.
S.S. Gershtein et al., Sov. J. Nucl. Phys. **48** (1988) 327.
C. Semay and B. Silvestre-Brac, ISN-93-69 (1993).

[2] W. Kwong and J.L. Rosner, Phys. Rev. **D44**(1991) 212.

[3] E. Eichten and C. Quigg, Phys. Rev. **D49** (1994) 5845.

[4] E. Bagan et al., Z. Phys. **C64** (1994) 57.

[5] C.-H. Chang and Y.Q. Chen, Phys. Rev. **D46** (1992) 3845.

[6] R.M. Barnett et al., Review of Particle Physics, Phys. Rev. **D54** (1996) 1.

[7] E. Braaten, K. Cheung, T.C. Yuan, Phys. Rev. **D48** (1993) R5049.

[8] V.V. Kiselev, A.K. Likhoded, M.V. Shevlyagin, Phys. Atom. Nucl. **57** (1994) 689.

[9] C. Quigg, FERMILAB-Conf-93/265-T.

[10] T.C. Yuan, Phys. Rev. **D50** (1994) 5664.

[11] Y.Q. Chen, Phys. Rev. **D48** (1993) 5181.

[12] D. London, 'B decay in the standard model and beyond', Snowmass B Physics 1993,
UdeM-LPN-TH-93-178 (1993), hep-ph/9310294.

[13] C.H. Chang and Y.Q. Chen, Phys. Rev. **D49** (1994) 3399.

[14] M. Lusignoli and M. Masetti, Z. Phys. **C51** (1991) 549.
I.I. Bigi, CERN-TH.7282/94, UND-HEP-94-BIG06.

[15] A. Leike and R. Rückl, Nucl. Phys. (Proc. Supp.) **37B** (1994) 215.
V.V. Kiselev, IHEP 95-80, hep-ph/9507228.

[16] P. Aarnio et al., DELPHI Collaboration, Nucl. Instr. Meth. **A 303** (1991) 233.

[17] P. Abreu et al., Nucl. Instr. Meth. **A378** (1996) 57.

[18] P. Abreu et al., DELPHI Collaboration, Phys. Lett. **B 341** (1994) 109.

[19] ALEPH Collaboration, ICHEP Conference, Warsaw 1996 - PA01-069.

[20] G. Alexander et al., OPAL Collaboration, Z. Phys. **C70** (1996) 197.

[21] L3 Collaboration, ICHEP Conference, Warsaw 1996 - PA05-046.

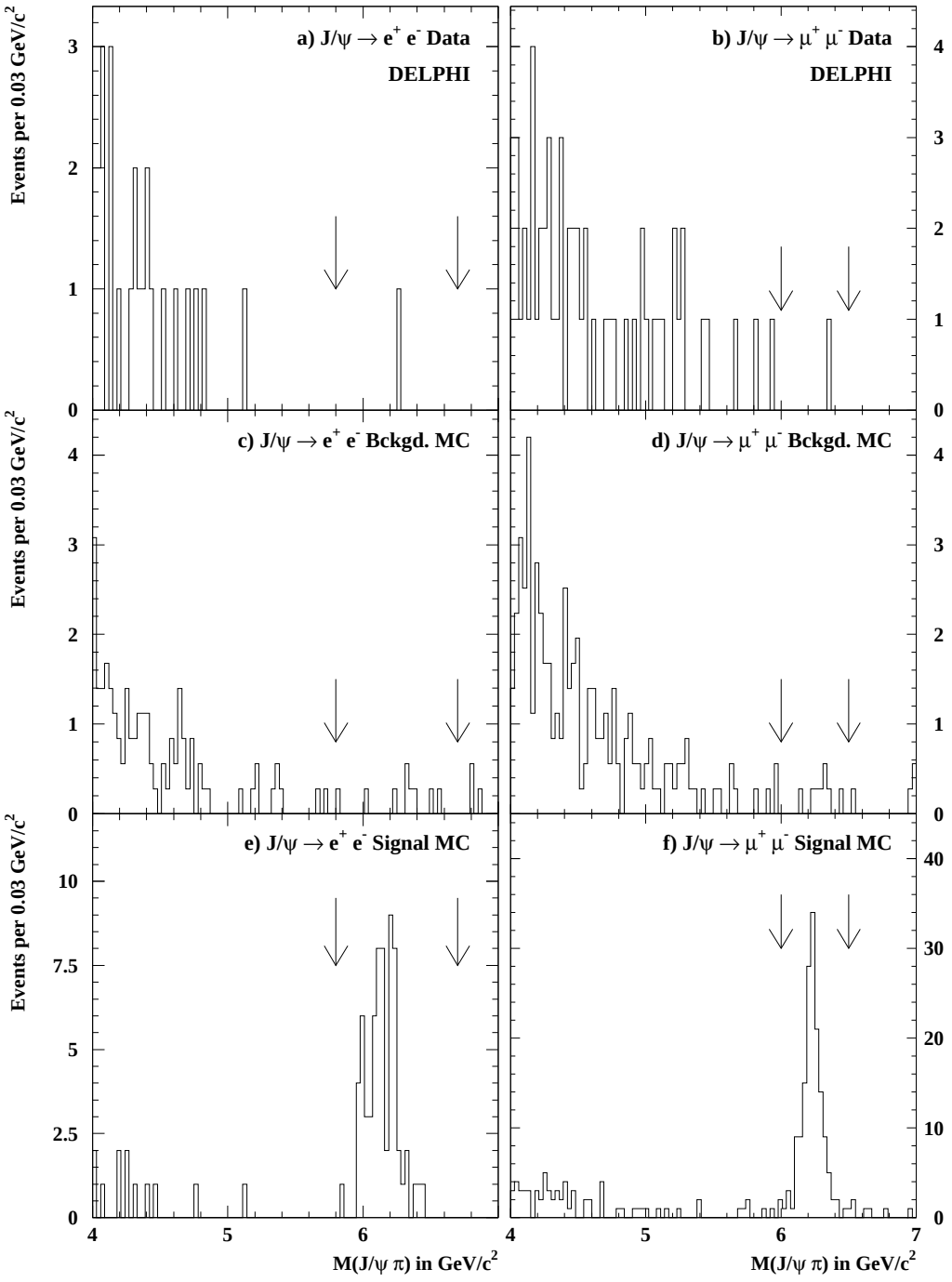

Figure 1: M($J/\psi\ \pi^{\pm}$) distributions - **a)** and **b)**: data for each J/ψ decay mode; **c)** and **d)**: simulated background normalised to the number of hadronics in the data; **e)** and **f)**: simulated signal. The arrows indicate the mass window for the $B_c{}^{\pm}$ search.

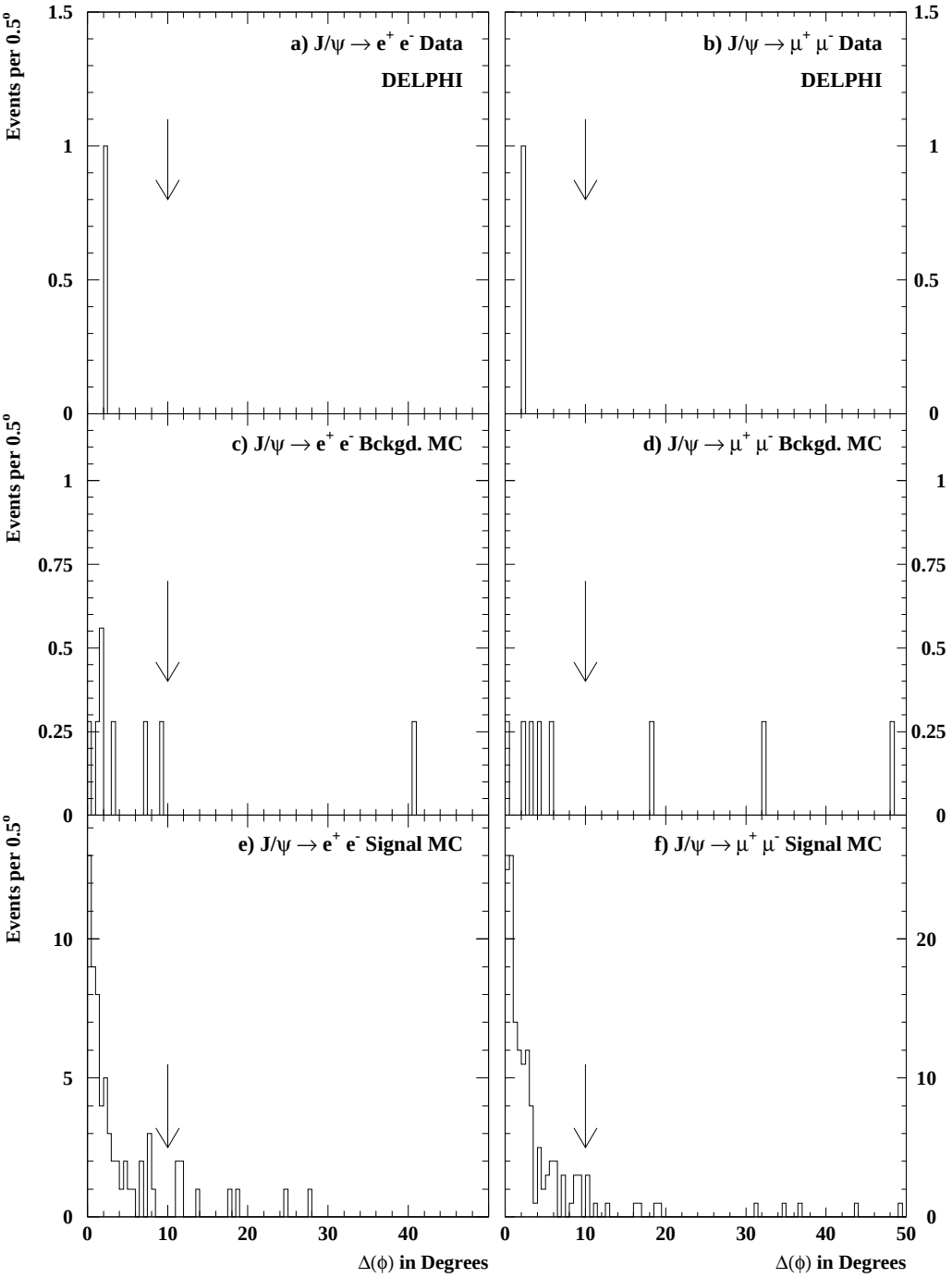

Figure 2: Distributions of the angle (in $R\Phi$) between the line joining the primary and secondary vertices and the momentum vector of the $(J/\psi\pi^{\pm})$ combination with mass in the search window - sub-plots a) to f) for event samples as in Fig. 1. The arrow indicates the upper limit for $B_c^{\pm} \rightarrow J/\psi\ \pi^{\pm}$ candidates.

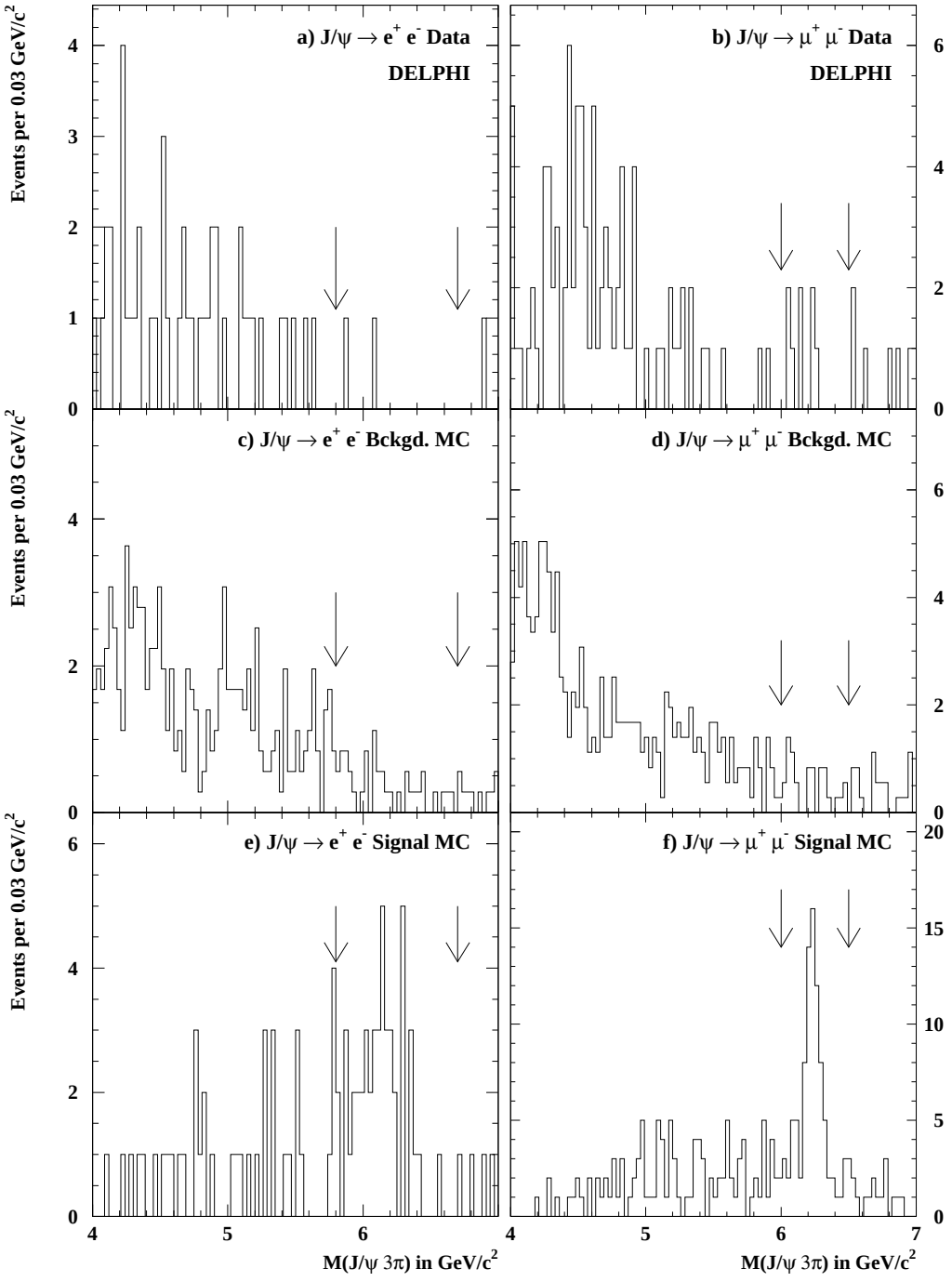

Figure 3: M(J/ψ $3(\pi)^{\pm}$) distributions - **a)** and **b)**: data for each J/ψ decay mode; **c)** and **d)**: simulated background normalised to the number of hadronics in the data; **e)** and **f)**: simulated signal. The arrows indicate the mass window for the $B_c{}^{\pm}$ search.

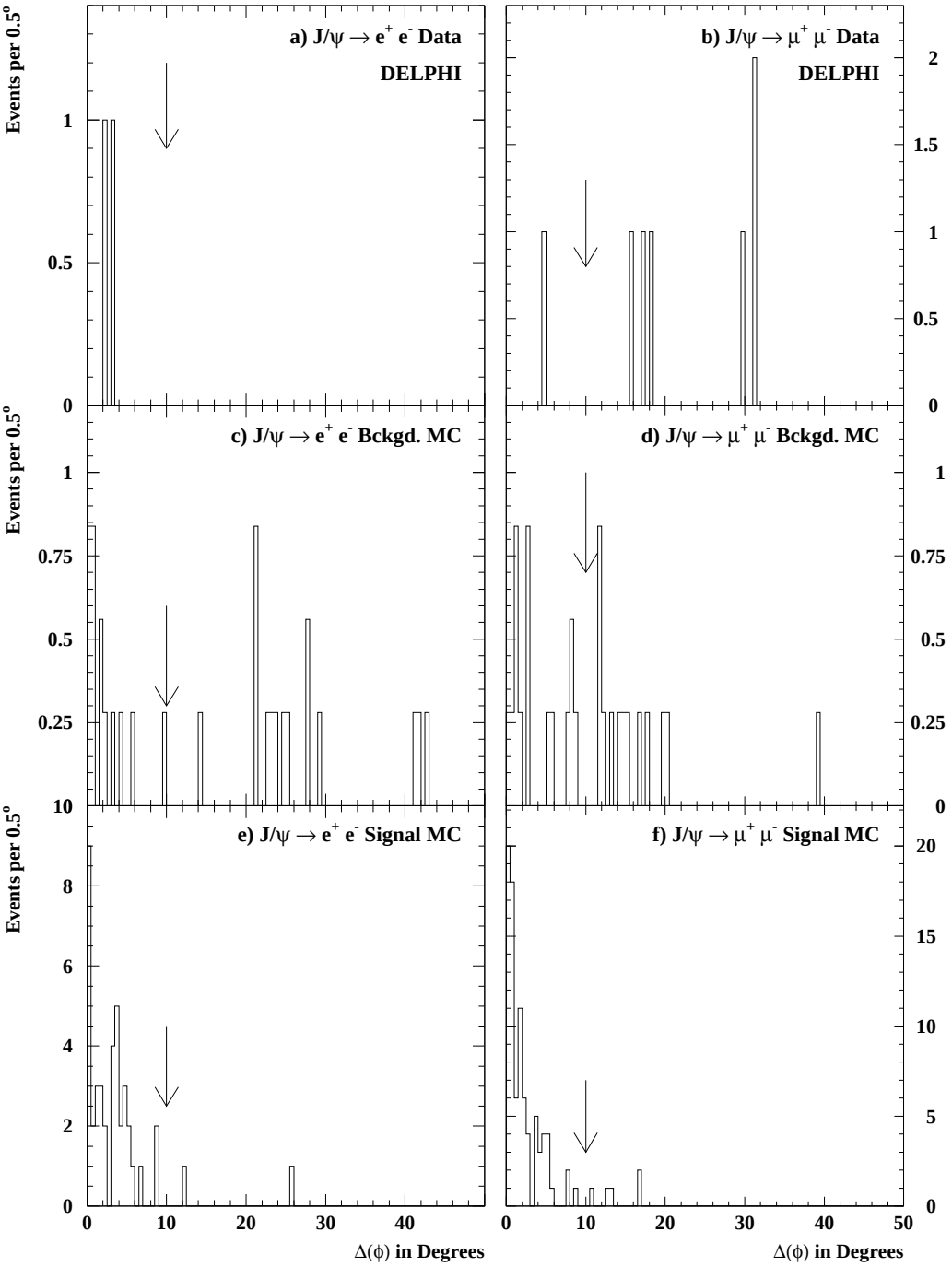

Figure 4: Distributions of the angle (in $R\Phi$) between the line joining the primary and secondary vertices and the momentum vector of the $(J/\psi\ 3\pi^{\pm})$ combination with mass in the search window - sub-plots a) to f) for event samples as in Fig. 3. The arrow indicates the upper limit for $B_c^{\pm} \rightarrow\ J/\psi\ 3(\pi)^{\pm}$.

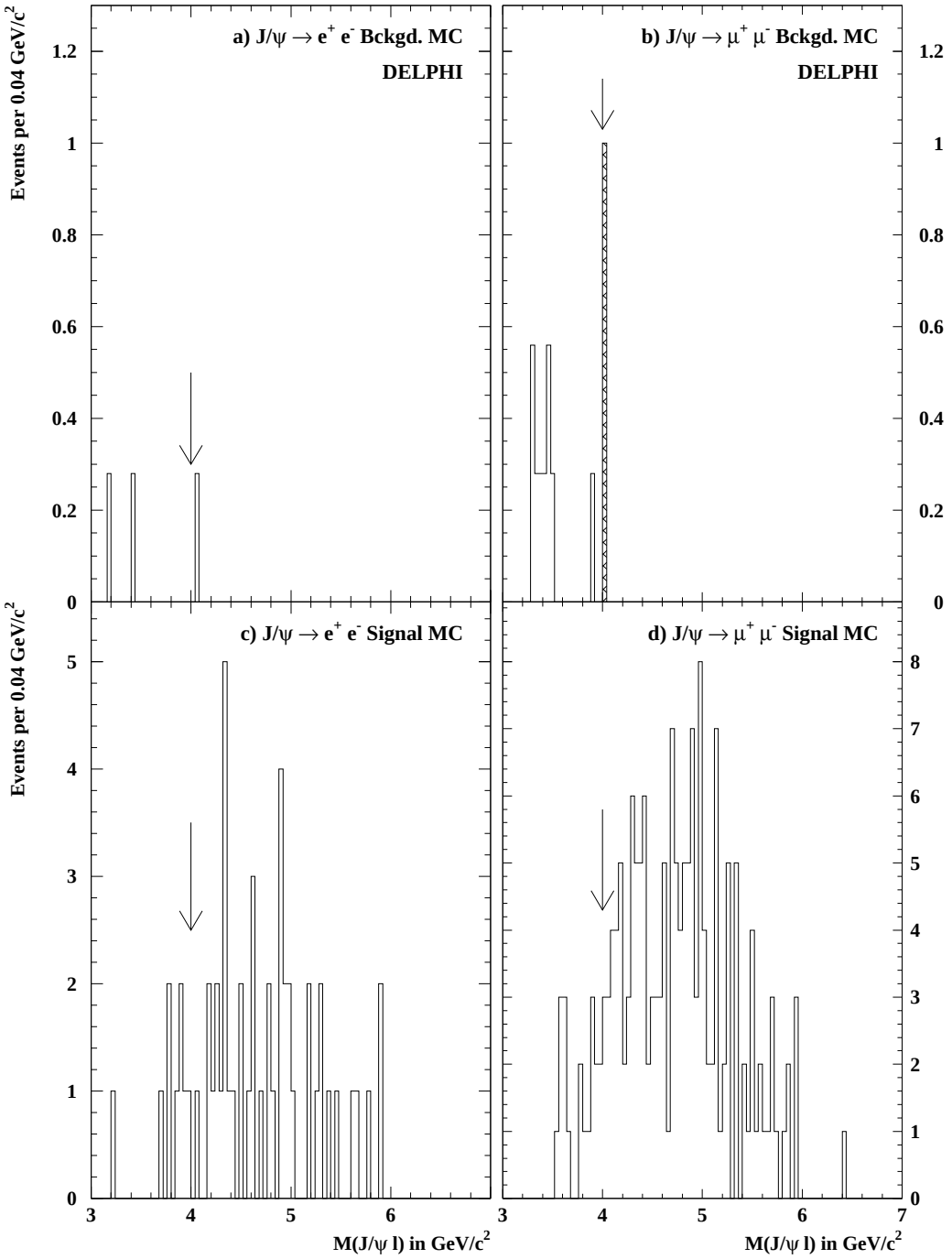

Figure 5: M($J/\psi\ \ell^{\pm}$) distributions - **a)** and **b)**: simulated background normalised to the data; **c)** and **d)**: simulated signal for each J/ψ decay mode. The single data event with $J/\psi \rightarrow \mu^+\mu^-$ is shown as the hatched histogram in b). The arrow indicates the lower limit for $B_c{}^{\pm}$ candidates.